

Figure 5.2 Phase-response curves: variation of the steady-state response phase with respect to the excitation frequency for different values of the damping ratio.

5.3 Amplitude and phase responses of the Duffing oscillator

In the previous section, the notions of slow and fast timescales, resonance, and secular terms were introduced. The addition of the nonlinear term y^3 to the simple *harmonic oscillator* – leading to the Duffing oscillator dramatically changes the picture. The principle of linear superposition can no longer be used to obtain the forced response of the linear system. In addition, the steady-state response depends on the initial conditions unlike that of the linear system where the steady-state response is independent of the chosen initial conditions. The maximum response also does not occur close to the system natural frequency as in the linear system. Due to the cubic nonlinearity, the system can experience resonances even when the excitation frequency is away from the natural frequency of the system. As the damped, forced nonlinear oscillator does not permit a closed-form solution, analytical approximations are sought for the forced response through perturbation analysis, as discussed in Chapter 4. The complexity of the response of the forced nonlinear oscillator is explored in the rest of this chapter.

Recognising the importance of the amplitude and phase responses of the linear oscillator, the same information is sought for the forced Duffing oscillator

$$\ddot{y} + 2\zeta \,\dot{y} + y + \gamma \,y^3 = F\cos\Omega \,t \tag{5.3.1}$$

As there is no closed form solution for Equation (5.3.1), perturbation analysis is used to determine an analytical approximation for the forced response, assuming that the system has weak nonlinearity and weak damping. The goal of this exercise is to understand the influence of nonlinearity and compare the behaviour of the forced nonlinear system with that of the forced linear system, whose behaviour was

discussed in the previous section. To facilitate the nonlinear analysis, a small parameter $\varepsilon \ll 1$, is introduced as an asymptotic ordering parameter and the damping and nonlinear terms are written, respectively, as $\zeta = \varepsilon \bar{\zeta}$ and $\gamma = \varepsilon \bar{\gamma}$, where $\bar{\zeta}$ and $\bar{\gamma}$ are O(1) quantities. With this rescaling, the unforced oscillator takes the following form:

$$\ddot{y} + y + \varepsilon \left(2\overline{\zeta}\,\dot{y} + \overline{\gamma}\,y^3\right) = 0\tag{5.3.2}$$

Examining Equation (5.3.2), it is clear that it is a perturbation of the corresponding undamped and unforced linear oscillator. In order to focus on the system response during a resonance excitation, a weak or soft forcing $F = \varepsilon \overline{F}$, where \overline{F} is O(1) is also assumed

With the assumptions of weak damping, weak nonlinearity, and weak forcing, Equation (5.3.1) can be rewritten as

$$\ddot{y} + y + \varepsilon (2\bar{\zeta}\,\dot{y} + \bar{\gamma}\,y^3) = \varepsilon \bar{F} \cos\Omega t \tag{5.3.3}$$

To find the different resonances possible in the system, a straightforward expansion of the following form is carried out:

$$y(t) = \varepsilon y_1(t) + \varepsilon^2 y_2(t) + \dots$$
 (5.3.4)

The expansion (5.3.4) is an example of a Poincaré asymptotic series. On substituting Equation (5.3.4) into Equation (5.3.3), collecting terms of the same order, and solving the differential systems that correspond to the orders $O(\varepsilon)$ and $O(\varepsilon^2)$, it is found that small divisor terms occur in the particular response at $O(\varepsilon)$ when

$$\Omega \approx 1 \tag{5.3.5a}$$

and at $O(\varepsilon^2)$ when

$$\Omega \approx 1/3$$
 or $\Omega \approx 3$ (5.3.5b)

Based on the order at which the small divisor terms occur, Equation (5.3.5a) is said to describe a primary resonance while conditions (5.3.5b) are said to describe secondary resonances. While the primary resonance is identical to the resonance relation observed in the corresponding linear system, the secondary resonances are particular to the nonlinear system. These resonances are also referred to as nonlinear resonances. The resonance associated with the case, where the system is forced close to 1/3 of the system natural frequency, is called a *superharmonic resonance*, while the resonance associated with the case, where the system is forced close to 3 times the system natural frequency, is called a *subharmonic resonance*.

5.3.1 Primary resonance

Next, the system response during the resonance excitation, $\Omega \approx 1$, is considered. The proximity of the excitation frequency to the system natural frequency is expressed as

$$\Omega = 1 + \varepsilon \sigma \tag{5.3.6}$$

where σ is called the *detuning parameter*, which is a measure of how close the excitation frequency is to the natural frequency. With the assumptions of weak damping, weak nonlinearity, and weak forcing close to the system natural frequency, Equation (5.3.1) is rewritten as

$$\ddot{y} + y + \varepsilon (2\bar{\zeta} \dot{y} + \bar{\gamma} y^3) = \varepsilon \bar{F} \cos((1 + \varepsilon \sigma)t) \tag{5.3.7}$$

Noting that the steady-state solution for the forced linear oscillator is $a\cos(\Omega t + \phi)$ (see Equation (5.2.7), for small ε , an analytical approximation for Equation (5.3.7) is assumed to have the form

$$y(t) = a(t)\cos(\Omega t + \phi(t)) + O(\varepsilon)$$
(5.3.8)

where the amplitude a and phase ϕ are slowly varying quantities. This analytical approximation is an example of a generalised asymptotic series, as the coefficients are also functions of the asymptotic ordering parameter, which is ε in this case. Such analytical approximations can be constructed by using the method of multiple scales or the method of averaging [8,9]. This construction is illustrated here by using the method of multiple scales. Let

$$y(t; \varepsilon) = y_0(T_0, T_1) + \varepsilon y_1(T_0, T_1) + \dots$$
 (5.3.9)

where the fast timescale T_0 and slow timescale T_1 are given by

$$T_0 = t, \quad T_1 = \varepsilon t \tag{5.3.10a,b}$$

With the introduction of the timescales, the time derivative with respect to time t is transformed as

$$\frac{d}{dt} = \frac{\partial}{\partial T_0} + \frac{\partial}{\partial T_1} = D_0 + D_1 \tag{5.3.11}$$

After substituting Equation (5.3.9) into Equation (5.3.7) and noting Equations (5.3.10a,b) and (5.3.11), the following hierarchy of equations can be obtained for O(1) and $O(\varepsilon)$, respectively.

$$D_0^2 y_0 + y_0 = 0, D_0^2 y_1 + y_1 = -2D_0 D_1 y_0 - 2\overline{\zeta} D_0 y_0 - \overline{\gamma} y_0^3 + \overline{F} \cos(T_0 + \sigma T_1)$$
(5.3.12a,b)

Then, the solution for the first component of the series (5.3.9) can be written as

$$y_0(T_0, T_1) = A(T_1)e^{jT_0} + A^*(T_1)e^{-jT_0}$$
 (5.3.13)

where $j = \sqrt{-1}$, $A(T_1)$ is a complex valued amplitude function, and * indicates a complex conjugate of that quantity. On substituting Equation (5.3.13) into Equation (5.3.12b), the result is

$$D_0^2 y_1 + y_1 = -j(2A' + 2\bar{\zeta}A)e^{jT_0} - 3\bar{\gamma}A^2A^*e^{jT_0} - \bar{\gamma}A^3e^{j3T_0} + \frac{\bar{F}}{2}e^{jT_0}e^{j\sigma T_1} + \text{c.c.} \quad (5.3.14)$$

where the prime indicates a time derivative with respect to the slow time T_1 and c.c. indicates the complex conjugate of the preceding terms. On setting the source of the secular terms to zero in Equation (5.3.14), the result is

$$-j(2A'+2\bar{\zeta}A)-3\bar{\gamma}A^2A^*+\frac{\bar{F}}{2}e^{j\sigma T_1}=0 \qquad (5.3.15)$$

Introducing the polar form of the complex amplitude

$$A(T_1) = \frac{1}{2}a(T_1)e^{i\beta(T_1)}$$
 (5.3.16)

where the amplitude $a(T_1)$ and the angle $\beta(T_1)$ are real-valued quantities, into Equation (5.3.15), separating the real and imaginary parts, and introducing the phase $\phi(T_1) = -(\sigma T_1 - \beta)$ leads to

$$a' = -\overline{\zeta}a - \frac{\overline{F}}{2}\sin\phi,$$

$$a\phi' = -\left(\sigma a - \frac{3}{8}\overline{\gamma}a^3 + \frac{\overline{F}}{2}\cos\phi\right)$$
(5.3.17a,b)

These equations, which describe the slow time evolutions of the amplitude and phase, are referred to as the modulation equations, slow-flow equations or averaged equations. The *fixed points* of Equation (5.3.17a,b) correspond to solutions with constant amplitude and phase. These solutions satisfy

$$\bar{\zeta}a + \frac{\bar{F}}{2}\sin\phi = 0,$$

$$\sigma a - \frac{3}{8}\bar{\gamma}a^3 + \frac{\bar{F}}{2}\cos\phi = 0$$
(5.3.18a,b)

or equivalently,

$$\begin{split} & \frac{\overline{F}}{2} \sin \phi = -\overline{\zeta} a, \\ & \frac{\overline{F}}{2} \cos \phi = -a \left(\sigma - \frac{3}{8} \overline{\gamma} a^2 \right) \end{split} \tag{5.3.19a,b}$$

Squaring and adding the equations in (5.3.19a,b) yields the frequency-response equation (amplitude–frequency equation)

$$\bar{F}^2 = 4a^2 \left(\bar{\zeta}^2 + \left(\sigma - \frac{3}{8} \bar{\gamma} a^2 \right)^2 \right)$$
 (5.3.20)

With this, the amplitude response (magnification factor) can be obtained as

$$M = \frac{a}{|\bar{F}|} = \frac{1}{2\sqrt{\bar{\zeta}^2 + (\sigma - \frac{3}{8}\bar{\gamma}a^2)^2}}$$
 (5.3.21)

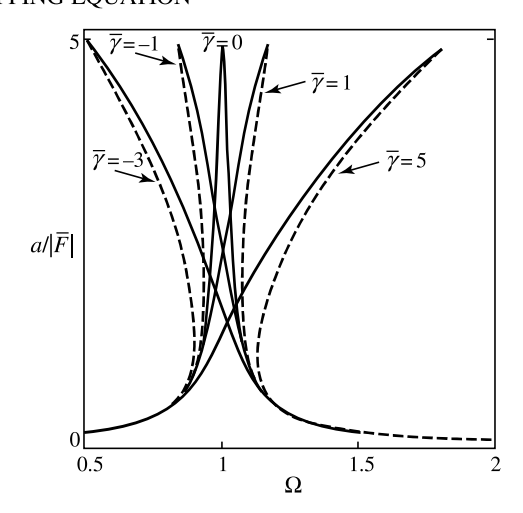


Figure 5.3 Amplitude-response curves for a varying strength of nonlinearities $\bar{\gamma}$ (from left to right). The parameter values used to construct these response curves are $\bar{F} = 0.3$, $\bar{\zeta} = 0.1$ and $\varepsilon = 0.2$.

In Figure 5.3 the amplitude-response curves for nonlinearities of different strengths $\overline{\gamma}$ are shown. Unlike the amplitude response in the linear case, the amplitude response in the nonlinear case can be multivalued. For negative values of $\overline{\gamma}$, the response curves lean toward the lower frequencies, resulting in a softening response. The more positive the nonlinearity, the higher is the shift of the peak value of the magnification factor away from $\Omega=1$ towards higher frequencies.

This is the hallmark of a hardening response. Increasing \bar{F} results in a harder (for positive $\bar{\gamma}$) or a softer (for negative $\bar{\gamma}$) characteristic. As discussed later in this section, the amplitude of the peak response is given by $\bar{F}/(2\bar{\zeta})$, and as the excitation amplitude is increased, this peak amplitude increases, and the corresponding response curve leans further to the right (left) of $\Omega = 1$ for positive (negative) $\bar{\gamma}$.

The influence of damping on the magnification factor is illustrated in Figure 5.4. The phase response of the Duffing oscillator is obtained from Equation (5.3.19) as

$$\tan \phi = \frac{\overline{\zeta}}{\sigma - \frac{3}{8}\overline{\gamma}a^2} \tag{5.3.22}$$

Phase-response curves are plotted in Figure 5.5 for the damping coefficients used in Figure 5.4. As is evident from Equation (5.3.22), the nonlinearity affects the phase response, which is now a function of the response amplitude; this dependence on the response amplitude distorts the shape of the phase-response curve.

A profound difference between the responses of the linear oscillator and that of the Duffing oscillator is that the response of the latter is multivalued; that is, for a fixed value of the driving frequency there can be as many as three different response amplitudes, as seen in Figures 5.3–5.5. This is a consequence of the fact that

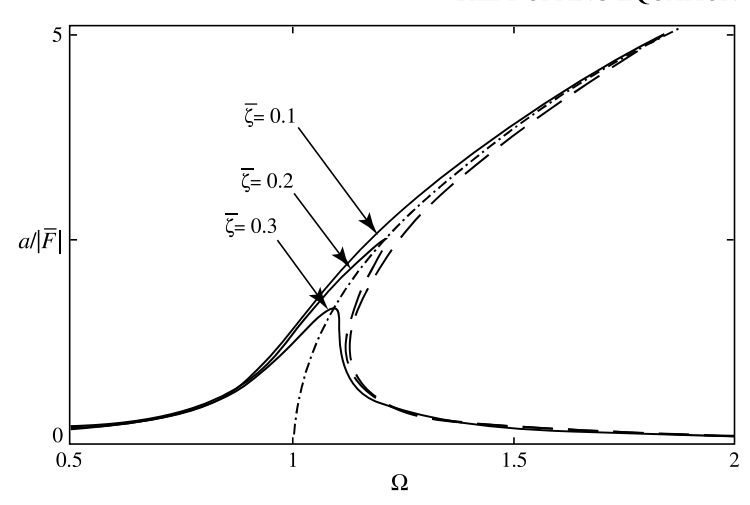


Figure 5.4 Amplitude-response curves: variation of the amplitude response with respect to the excitation frequency for different values of the damping ratio $\bar{\zeta}$. The parameter values used to construct these response curves are $\bar{F}=0.3$, $\varepsilon=0.2$ and $\bar{\gamma}=5$. The backbone curve is shown as a dotted line.

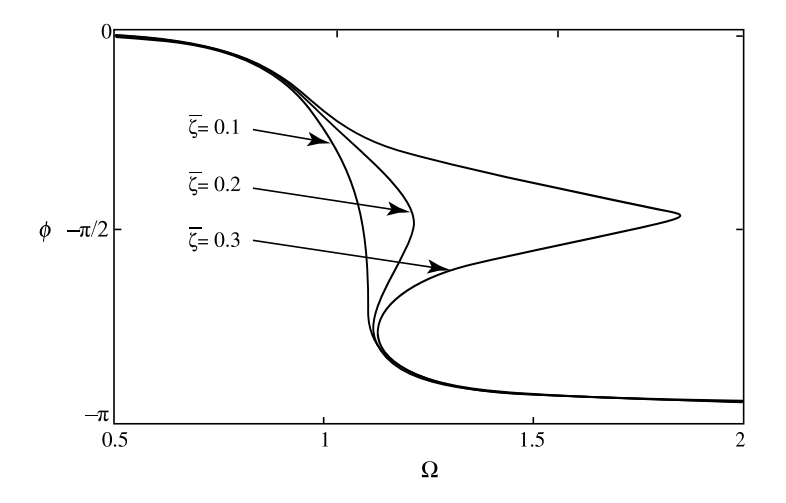


Figure 5.5 Phase-response curves: variation of the phase response with respect to the excitation frequency for different values of the damping ratio $\bar{\zeta}$. The parameter values used to construct these response curves are $\bar{F}=0.3$, $\varepsilon=0.2$ and $\bar{\gamma}=5$.

Equation (5.3.20) is a cubic equation in a^2 . Similar to the case of the linear oscillator, the maximum value of the magnification factor can be found from

$$\frac{dM}{d\Omega} = 0 \quad \text{and} \quad \frac{d^2M}{d\Omega^2} < 0 \tag{5.3.23a,b}$$

Differentiating Equation (5.3.20) with respect to Ω yields

$$\frac{1}{32\varepsilon^2}a\left(3\bar{\gamma}\varepsilon a^2 - 8\Omega + 8\right)\left(3a\bar{\gamma}\varepsilon\frac{da}{d\Omega} - 4\right) + \left(\bar{\zeta}^2 + \left(\frac{\Omega - 1}{\varepsilon} - \frac{3a^2\bar{\gamma}}{8}\right)^2\right)\frac{da}{d\Omega} = 0$$
(5.3.24)

which can be solved for $da/d\Omega$ as

$$\frac{da}{d\Omega} = \frac{8a(3\overline{\gamma}\varepsilon a^2 - 8\Omega + 8)}{27\overline{\gamma}^2\varepsilon^2 a^4 - 96\overline{\gamma}\varepsilon(\Omega - 1)a^2 + 64\left(\varepsilon^2\overline{\zeta}^2 + (\Omega - 1)^2\right)}$$
(5.3.25)

This derivative vanishes (and so does $dM/d\Omega$) when

$$3\bar{\gamma}\varepsilon a^2 - 8\Omega + 8 = 0 \Rightarrow a_{\rm p} = \sqrt{\frac{8(\Omega - 1)}{3\varepsilon\bar{\gamma}}} = \sqrt{\frac{8(\Omega - 1)}{3\gamma}}$$
 (5.3.26a)

which on the basis of Equations (5.3.6) and (5.3.20) can be rewritten as

$$a_{\rm p} = \sqrt{\frac{8\varepsilon\sigma}{3\varepsilon\bar{\gamma}}} = \sqrt{\frac{8\sigma}{3\bar{\gamma}}} = \frac{\bar{F}}{2\bar{\zeta}}$$
 (5.3.26b)

From Equations (5.3.26a) and (5.3.26b), it follows that

$$M_{\rm p} = \frac{a_p}{|\bar{F}|} = \frac{\sqrt{\frac{8(\Omega - 1)}{3\varepsilon\bar{\gamma}}}}{|\bar{F}|} = \frac{\sqrt{\frac{8(\Omega - 1)}{3\gamma}}}{|\bar{F}|}$$
(5.3.27a)

and

$$M_{\rm p} = \frac{a_p}{|\bar{F}|} = \frac{1}{2\bar{\zeta}}$$
 (5.3.27b)

respectively. Equation (5.3.26a) describes the so-called *backbone curve*, which is also plotted in Figure 5.4. From Equations (5.3.26b) and (5.3.27b), it follows that the peak amplitude and the associated magnification factor are independent of the strength of the nonlinearity $\bar{\gamma}$ (however, this is only true for weak nonlinearity. The peak amplitude actually decreases for a hardening nonlinearity and increases for a softening nonlinearity. This is discussed in more detail in [10]). This is evident in Figure 5.3, where all of the peaks have the same magnitude for a fixed forcing amplitude and constant damping ratio. However, the peak amplitude location that can

be determined from Equation (5.3.26b) as

$$\sigma_{\rm p} = \frac{3\overline{\gamma}}{8} \left(\frac{\overline{F}}{2\overline{\zeta}}\right)^2 \tag{5.3.27c}$$

depends on the strength of the nonlinearity.

In Figure 5.6, a representative amplitude-response curve is shown to illustrate the jump phenomenon. There is exactly one solution branch for $\Omega < \Omega_1, \Omega_2 < \Omega$ and three coexisting solutions for $\Omega_1 < \Omega < \Omega_2$, the so-called interval of bistability. At the frequency location $\Omega = \Omega_1$ ($\Omega = \Omega_2$), there are only two solutions S_1 and S_2 (S_3 and S_4), since at this frequency location the two solution branches merge. At $\Omega = \Omega_1$ and Ω_2 , the periodic response of the forced Duffing oscillator loses *stability*, leading to a jump in the response, as discussed later.

In Figure 5.7, a representative solution of the Duffing equation is shown for specific initial conditions. As the harmonically forced oscillator is a second-order nonautonomous system, there are trajectory crossings in the (y, \dot{y}) plane. Although there is a unique solution associated with any initial condition, for some system and excitation parameter values, more than one solution satisfying Equation (5.3.3) can exist; that is, trajectories initiated from different initial conditions can be attracted to different solutions. Coexisting solutions are illustrated in Figure 5.8. These solutions are marked as P and Q in Figure 5.6. To elucidate the importance of several coexisting solutions, Figure 5.6 is revisited. Assume that an experiment is conducted. As the

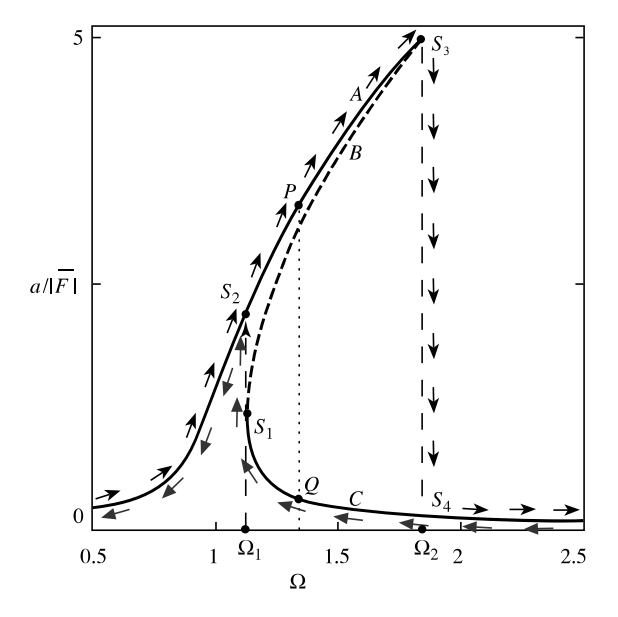


Figure 5.6 Illustration of the jump phenomenon or hysteresis in the response of the Duffing oscillator (5.3.3). The parameter values used to construct these response curves are $\overline{F} = 0.3$, $\overline{\zeta} = 0.1$, $\varepsilon = 0.2$ and $\overline{\gamma} = 5$. Phase plots corresponding to points P and Q are shown in Figure 5.8.

152 THE DUFFING EQUATION

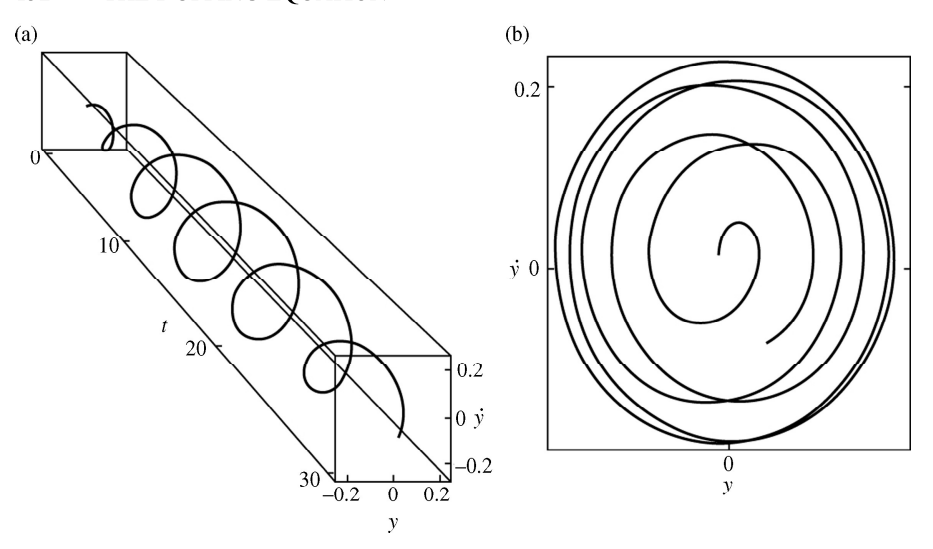


Figure 5.7 (a) System response in the (y,\dot{y},t) space and (b) the phase plot in the (y,\dot{y}) plane for $\bar{F}=0.3$, $\bar{\zeta}=0.1$, $\varepsilon=0.2$, $\bar{\gamma}=5$ and $\Omega=1.2$ over the time interval of $0 \le t \le 30$. The initial conditions are $y_0=0.01$, $\dot{y}_0=0$.

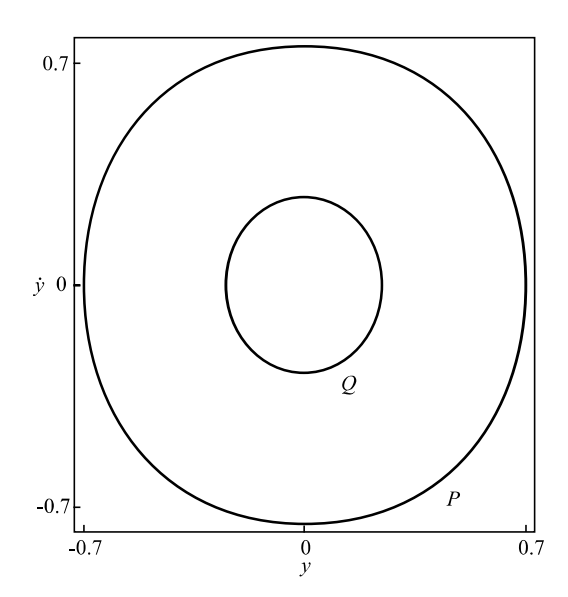


Figure 5.8 Phase plot of coexisting stable steady-state solutions in the (y, \dot{y}) plane for $\bar{F}=0.3, \ \bar{\zeta}=0.1, \ \epsilon=0.2, \ \bar{\gamma}=5$ and $\Omega=1.34$.

driving frequency – a natural control parameter – is gradually increased from $\Omega < \Omega_1$ in a quasistatic manner, the response amplitude will follow the upper branch or the large amplitude solution branch of the response diagram. Once Ω_2 is reached, this large amplitude forced vibration ceases to exist, and a fast (compared to the dominant timescale of the system) transition takes place to the lower branch consisting of small amplitude solutions; that is, a jump occurs from a large amplitude solution branch to a small amplitude solution branch. As the driving frequency Ω is further increased, the response follows the small amplitude solution branch. If the driving frequency is now slowly decreased from a frequency $\Omega > \Omega_2$, the amplitude of the steady-state forced response increases in accordance with the lower branch or the small-amplitude solution branch. At $\Omega = \Omega_1$, a transition occurs to a solution on the upper branch.

The transitions from the upper branch to the lower branch and vice versa occur at different values of the driving frequency, and as a consequence, depending on how the specific driving frequency is reached in the range of $\Omega_1 < \Omega < \Omega_2$, the response is different since it depends on the initial conditions; this phenomenon is called *hysteresis*.

In a physical experiment, the middle solution branch (the branch that joins the upper or large-amplitude solution branch and the lower or small amplitude solution branch) is not observed. The solutions on this middle solution branch are unstable, which means that if solutions on this middle branch are perturbed they will not return to that solution, but will be attracted to another solution. In the following, the stability of the solutions is examined.

To find the values of the critical points Ω_1 and Ω_2 , the authors utilise the fact that these points correspond to vertical tangencies of the response curve; that is, where $d\Omega/dM=0$. This condition can be found by equating the denominator of Equation (5.3.25) to zero, which translates to

$$27\overline{\gamma}^2 \varepsilon^2 a^4 - 96\overline{\gamma} \varepsilon (\Omega - 1)a^2 + 64\left(\varepsilon^2 \overline{\zeta}^2 + (\Omega - 1)^2\right) = 0$$
 (5.3.28)

whose roots provide

$$\Omega_{1,2} = \frac{1}{8} \left(8 + 6\bar{\gamma}\varepsilon a^2 - \varepsilon \sqrt{9a^4\bar{\gamma}^2 - 64\bar{\zeta}^2} \right)$$
 (5.3.29)

The condition for the existence of real solutions is

$$a \ge \sqrt{\frac{8\overline{\zeta}}{3\overline{\gamma}}} \tag{5.3.30}$$

The onset of bistability is characterised by the limiting case $a=\sqrt{8\overline{\zeta}/(3\overline{\gamma})}$. This corresponds to $\Omega_1=\Omega_2=1+2\varepsilon\overline{\zeta}$, and the critical forcing amplitude $\overline{F}=8\sqrt{\overline{\zeta}\left(\overline{\zeta}^2+2\overline{\gamma}\overline{\zeta}+2\overline{\gamma}^2\right)/3\overline{\gamma}}$.

To characterise the stability of the solution branches depicted in Figure 5.6, the stability properties of the fixed points (a, ϕ) of Equations (5.3.17) need to be

understood. The Jacobian matrix of this flow is

$$\mathbf{J} = \begin{bmatrix} -\overline{\zeta} & a\left(\sigma - \frac{3}{8}\overline{\gamma}a^2\right) \\ -\left(\sigma - \frac{9}{8}\overline{\gamma}a^2\right) & -\overline{\zeta} \end{bmatrix}$$
 (5.3.31)

whose trace tr **J** and determinant Δ are given by

tr
$$\mathbf{J} = -2\overline{\zeta}$$
,

$$\Delta = \overline{\zeta}^2 + \left(\sigma - \frac{9}{8}\overline{\gamma}a^2\right)\left(\sigma - \frac{3}{8}\overline{\gamma}a^2\right)$$
(5.3.32a,b)

respectively. The trace is equal to the sum of the eigenvalues of the Jacobian matrix J, while the determinant Δ is equal to the product of its eigenvalues.

For the damped system, the trace, and thus, the sum of the eigenvalues of the Jacobian is negative, and therefore at least one of the eigenvalues has a negative real part. If the other eigenvalue has a negative (positive) real part, then, the fixed point (a, ϕ) is a stable node (saddle point). Branches of stable and unstable fixed points are shown as solid and dashed lines, respectively, in Figures 5.3, 5.4 and 5.6. If the other eigenvalue becomes zero, the system undergoes a static *bifurcation* (i.e., *saddle-node* or *pitchfork bifurcation*), but dynamic bifurcations such as *Hopf bifurcations* are not possible, as also discussed in Chapter 3. The condition for having a zero eigenvalue can be derived from Equations (5.3.32) and (5.3.20) (condition for the existence of a fixed point and one of the eigenvalues of the Jacobian matrix is zero)

$$\Delta = \overline{\zeta}^2 + \left(\sigma - \frac{9}{8}\overline{\gamma}a^2\right)\left(\sigma - \frac{3}{8}\overline{\gamma}a^2\right) = 0,$$

$$\overline{F}^2 = 4a^2\left(\overline{\zeta}^2 + \left(\sigma - \frac{3}{8}\overline{\gamma}a^2\right)^2\right)$$
(5.3.33a,b)

This provides the following simple relationship between the system parameters at the static bifurcation point

$$\bar{F}^2 = 3\bar{\gamma}a^4 \left(\sigma - \frac{3}{8}\bar{\gamma}a^2\right) \tag{5.3.34}$$

Having explored the stability of the solutions, the domains of attraction for the stable solutions are now discussed for the excitation parameter values corresponding to which three solutions exist. Let the stable fixed points A and C of Equation (5.3.17a,b) correspond to the upper branch and lower branch of solutions of Figure 5.6 for a certain set of parameter values, and the unstable fixed point B correspond to the middle branch of solutions for these parameter values. The unstable fixed point is a saddle point, and there is a one-dimensional *stable manifold W*^S associated with the eigenvalue with the

negative real part and a one-dimensional *unstable manifold* W^U associated with the eigenvalue with the positive real part. It is noted that a stable manifold is tangent to the eigenvector associated with the eigenvalue with the negative real part, and any trajectory initiated on the stable manifold is attracted to B as $t \to \infty$. An unstable manifold is tangent to the eigenvector associated with the eigenvalue with the positive real part, and any trajectory initiated on the unstable manifold is attracted to B as $t \to -\infty$. A representative illustration of these manifolds is given in Figure 5.9 in the (a, ϕ) plane.

The stable manifold of *B* partitions this plane into two regions, which are the basins of attraction of the stable fixed points *A* and *C*. Depending on the initial conditions, the trajectories are attracted to either point *A* or *C*, as $t \to \infty$.

So far, the driving frequency has been considered as the control (bifurcation) parameter. An alternative way to capture the dynamics of the system is to find the amplitude of the response as the function of the amplitude of the driving force. The so-called force-response curve is depicted in Figure 5.10. Here, again, multiple and up to three coexisting solutions (the solid and dashed lines correspond to stable and unstable branches, respectively) can be observed. As F is increased quasi-statically and then decreased, a hysteresis phenomenon is seen as earlier noted in the context of Figure 5.6. In particular, there are three coexisting solutions for $F_1 < F < F_2$, and exactly one solution branch outside this region of bistability. The stable (thick solid line) and unstable (thick dashed line) branches merge at $F = F_1$ and $F = F_2$. At these points there is a *jump*, labelled by a thin dashed line, in the response.

The qualitative change or bifurcation associated with the jump phenomenon is an example of a catastrophic bifurcation (see, for example, [7]) since the states of the system vary discontinuously as the control parameter is varied gradually through its critical value. In the present case, the postbifurcation response is a bounded *attractor*, to be specific, a periodic attractor. However, this may not be true in all situations. It is noted that the jump phenomenon is related to the cusp catastrophe (see, for example, [2]) which is one of many elementary catastrophes proposed nearly four

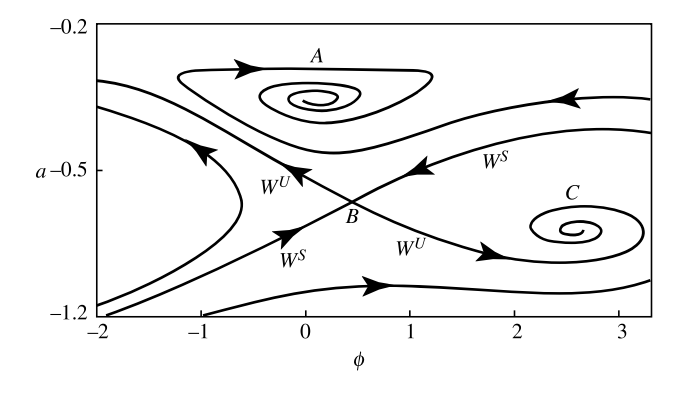


Figure 5.9 Phase plane for Equation (5.3.17a,b) with three coexisting equilibrium solutions. The stable manifold W^S of the saddle point B separates the domains of attraction of A and C. $\bar{F} = 0.3$, $\bar{\zeta} = 0.1$, $\varepsilon = 0.2$, $\bar{\gamma} = 5$ and $\Omega = 1.2$.

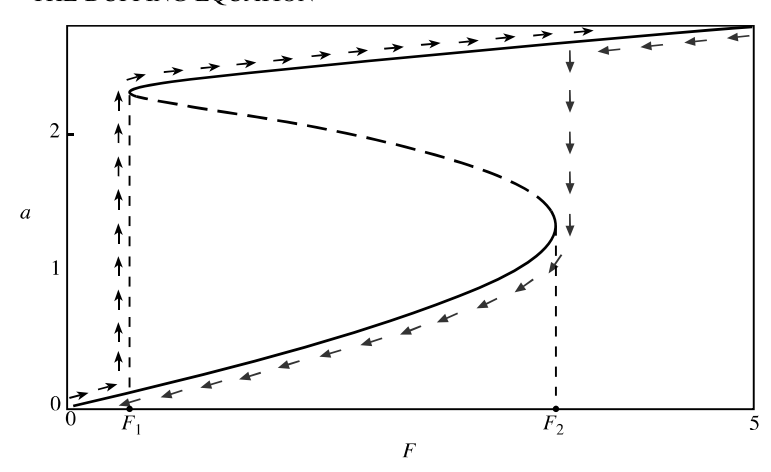


Figure 5.10 Force-response curve for $\bar{\zeta} = 0.1$, $\varepsilon = 0.1$, $\bar{\gamma} = 1$ and $\Omega = 1.2$.

decades ago [11]. Holmes and Rand [12] were the first to apply catastrophe theory to the Duffing oscillator.

Catastrophe theory is based on the behaviour of canonical functions of the form

$$f(y,\mu) = 0 (5.3.35)$$

close to the singular or critical point y = 0 at the control parameter value $\mu = 0$ of the system. The fixed-point equations given by Equation (5.3.18a,b) are in the form of Equation (5.3.35), and the jump location corresponds to a singular or critical point of this system. The theory of singularities, which encompasses catastrophe theory, can be used to understand the structural stability of bifurcations; that is, to understand whether a certain bifurcation would be stable to a perturbation to the system. For instance, this theory can be used to answer the question of whether the jump phenomenon seen in Figure 5.10 would still persist if a perturbation in the form of nonlinear viscous damping is added to the system described by Equation (5.3.7).

The analysis and numerical results discussed thus far are valid for a weakly nonlinear system subjected to a soft forcing at a primary resonance (i.e., $\Omega = 1$) of the system. Subsequently, the cases of secondary resonances are analysed.

5.3.2 Secondary resonances

Due to the cubic nonlinearity in the system there are also resonances at other frequencies as mentioned earlier. These secondary resonances, occur at $\Omega=1/3$ and $\Omega=3$, which are different cases of the resonance relation $\Omega=(1-m)/n$, where m and n are integers such that |m|+|n|=3. Weakly nonlinear analyses can also be carried out to determine the system response as discussed in [2,7–9]. To illustrate this, the following system is considered

$$\ddot{y} + \varepsilon 2\bar{\zeta} \dot{y} + y + \varepsilon \gamma y^3 = F \cos \Omega t \tag{5.3.36}$$